American Mineralogist, Volume 73, pages 97–104, 1988

Location of trace Fe^{3+} ions in sanidine, $KAlSi_3O_8$

Ivan Petrov, S. S. Hafner
Institut für Mineralogie der Universität Marburg, Lahnberge, 3550 Marburg, West Germany

Abstract

Electron paramagnetic resonance of single crystals of sanidine was studied at frequencies of the X band (~9.5 GHz) between 4.2 K and 295 K and the Q band (~35 GHz) at 295 K. Five broad resonance lines at $g_{eff} \approx 7.9$, $g_{eff} \approx 4.3$, and $g_{eff} \approx 3.7$ (X band) and at $g_{eff} \approx 2.04$ and $g_{eff} \approx 2.003$ (Q band) were identified. These five g values refer to the orientation **B** parallel to **c***. The lines at $g_{eff} \approx 4.3$ and $g_{eff} \approx 3.7$ result from transitions $m_s = \pm 3/2$, those at $g_{eff} \approx 7.9$ from the transition $m_s = 5/2 \rightarrow 3/2$, and those at $g_{eff} \approx 2.045$ and $g_{eff} \approx 2.003$ to transitions $m_s = \pm 1/2$. These five lines are due to Fe^{3+} at the tetrahedral positions T1 and T2 of sanidine. The lines $g_{eff} \approx 4.3$ and $g_{eff} \approx 2.003$ were assigned to the position T1, the lines $g_{eff} \approx 3.7$ and $g_{eff} \approx 2.045$ to the position T2. The parameters $\lambda = E/D$ were estimated: $\lambda \approx 0.32$ for T1 and $\lambda \approx 0.22$ for T2. An additional, very weak resonance line at $g_{eff} \approx 6$ (**B** parallel to **a**) in the Q band was attributed to $Fe^{3+}O_3OH$ substitutions at T1 and/or T2, in agreement with a value $\lambda \approx 0$ indicating pseudotrigonal symmetry.

Fe^{3+} ions in sanidine are disordered over the T1 and T2 positions but show some preference for T1. The kinetics for $Fe^{3+} \leftrightarrow Al^{3+}$ as well as $Fe^{3+} \leftrightarrow Si^{4+}$ exchange appear to be slow, possibly slower than the exchange of Al and Si between these positions.

Introduction

In the past three decades, order-disorder of (Al^{3+},Si^{4+}) over the four distinct tetrahedral positions T1(O), T1(m), T2(O), and T2(m) in alkali feldspars has been discussed extensively in many publications. Although important aspects of this phenomenon may now be clarified, other questions—e.g., quantitative data on the kinetics of the Al ↔ Si exchange among the tetrahedral positions—are still open. However, almost no information is available at this time on the kinetics of trace ions substituted for Al or Si at these sites. A possible trace ion substituted for Al^{3+} is Fe^{3+}, which is found in almost every feldspar in small amounts. It was shown by electron paramagnetic resonance (EPR) that in low microcline and low albite, Fe^{3+} only occurs at one tetrahedral position, which may be assigned to the position T1(O) of Al^{3+} (Marfunin et al., 1967; Gaite and Michoulier, 1970; Michoulier and Gaite, 1972; Matyash et al., 1981). No details are known yet on the distribution of Fe^{3+} over distinct tetrahedral positions in more or less disordered alkali feldspars, as, for example, sanidine. Moreover, no information is available on the kinetics of possible $Fe^{3+} \leftrightarrow Al^{3+}$ and $Fe^{3+} \leftrightarrow Si^{4+}$ exchange reactions. For example, it is not known whether the $Fe^{3+} \leftrightarrow Si^{4+}$ exchange is generally faster or slower than the $Al^{3+} \leftrightarrow Si^{4+}$ exchange in alkali feldspars.

Sanidine is monoclinic (space group $C2/m$), i.e., crystallographically, t1(O) = t1(m) = t1, and t2(O) = t2(m) = t2. Here, t1(O), etc., refer to the site occupancy of Al at position T1(O), etc., respectively. The distribution of Al and Si over T1 and T2 is generally disordered although small degrees of partial order may be observed in certain sanidines, Al somewhat preferring T1 and Si somewhat preferring T2, without violation of the monoclinic symmetry.

In this paper we present some data obtained from EPR spectra of single crystals of sanidine taken at frequencies in the X and Q bands. The primary intention was to find the assignment of the paramagnetic centers produced by substituted Fe^{3+} ions on the crystallographic positions, which has to be the basis for any kinetic study from EPR spectra.

Spin Hamiltonian of d^5 systems

For comprehensive representation of the spin Hamiltonian for Fe^{3+} (d^5) in a noncubic crystalline electric field (CEF), the reader is referred to the studies of Castner et al. (1960), Troup and Hutton (1964), Wickman et al. (1965), and Dowsing and Gibson (1969). Here, the effect of CEF is considered briefly as far as it applies to the present study. The CEF, which causes the spin to align along a preferred crystalline direction in the absence of a static magnetic field, may be described by the last two terms (i.e., the "fine structure" terms) in the spin Hamiltonian (Brodbeck 1980),

$$\hat{H} = \mathbf{g}\beta\mathbf{BS} + D[S_z^2 - \tfrac{1}{3}S(D+1)] + E(S_x^2 - S_y^2), \quad (1)$$

where x, y, and z are axes related to the CEF at the Fe^{3+} ion. β is the Bohr magneton, **S** the effective spin of Fe^{3+}, **g** the electronic g factor, i.e., a tensor of second rank with the eigenvalues g_x, g_y, g_z, and **B** the external magnetic field. The parameter $D = 3B_2^0$ measures the axially sym-

0003–004X/88/0102–0097$02.00

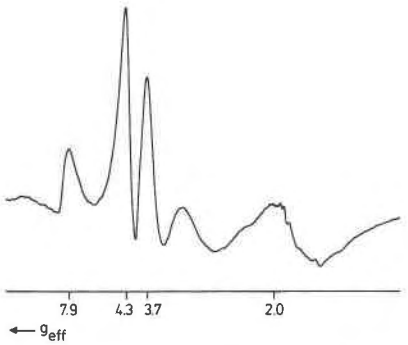

Fig. 1. EPR spectrum (X band) of a crystal of sanidine from Volkesfeld, $\nu = 9.3789$ GHz, $T = 295$ K. It shows three typical signals of Fe^{3+} at $g_{eff} \approx 7.9$, $g_{eff} \approx 4.3$, and $g_{eff} \approx 3.7$ in sanidine. Moreover, an additional line at $g_{eff} \approx 2$ is probably due to Fe^{3+} clusters. The external magnetic field **B** was parallel to the plane (010). The angle between **B** and **c*** was 20°.

metric part of the initial splitting; the parameter $E = B_2^2$ measures the part with orthorhombic symmetry. The orbital angular momentum of the Fe^{3+} (d^5) free ion is zero, and the ground state is sixfold degenerate, $S = 5/2$. If D and E are zero, an isotropic EPR line with a g value slightly greater than 2 is expected. Here, "isotropic" refers to invariance of field position with respect to the orientation of the crystal to **B**. If the CEF is large (D or $E \geq g\beta B$), the apparent g factor will be different from 2.

Two special cases of the CEF should be considered: $D \gg g\beta B$, $E = 0$; and $D = 0$, $E \gg g\beta B$. In the first case ($D \gg g\beta B$, $E = 0$) for $B = 0$, the six degenerate spin states of the free ion are split into three distinct Kramers doublets with the levels $m_s = \pm 5/2$, $\pm 3/2$, and $\pm 1/2$. The pair at the $m_s = \pm 1/2$ level is lowest for $D > 0$. If a small magnetic field is applied, each pair splits, but $\Delta m = \pm 1$ transitions are allowed only between the $m_s = \pm 1/2$ states. Resonance within the other two doublets is forbidden by the selection rule $\Delta m = \pm 1$. The observed g factor parallel to the z axis is $g_z = g\| = 2$. Perpendicular to the z axis, it is $g_x = g_y = g_\perp = 6$. For the second case ($D = 0$, $E \gg g\beta B$), there are again three Kramers doublets for $B = 0$. In case of a small B, they yield g factors with the principal values $g_z = 0.607$, $g_x = 0.857$, and $g_y = 9.678$ for the upper and lower doublets and an isotropic factor $g = g_x = g_y = g_z = 4.286$ for the central doublet. For the interpretation of the Fe^{3+} spectra of sanidine in the X-band spectrum, the second case was examined; in the Q-band spectrum, the first and the second cases were examined.

The effective local symmetry of the CEF at the site of the Fe^{3+} ion may be characterized by the ratio $E/D = B_2^2/3B_2^0 = \lambda$ (cf., e.g., Troup and Hutton, 1964; Hutton, 1969; Brodbeck, 1980), where λ may vary between 0 and 0.33. $\lambda = 0$ corresponds to the case of an axially symmetric CEF ($D \neq 0$, $E = 0$). Then, an increase in λ represents a deviation from axial symmetry toward orthorhombic symmetry. $\lambda = 0.33$ corresponds to the case of maximum possible orthorhombic symmetry with equally spaced Kramers doublets; values of λ nominally greater than 0.33 represent a convergence toward axial symmetry again. If $\lambda = 1$, the CEF is entirely axial. Gaite and Michoulier (1970) computed a relationship between g and λ that allows information on the deviation from axial symmetry of the site to be obtained from the observed resonance fields for feldspar.

Samples

The investigated crystals of sanidine were from a leucite phonolite tuff near Volkesfeld, Eifel, West Germany (Bank, 1967; Frechen, 1976). Crystals from this locality may exceed 20 cm in diameter. They are optically transparent, quite homogeneous, and smoky colored. Speit and Lehmann (1982) suggested that the smoky color is produced by an electron hole on the oxygen anion between two adjacent Al cations (Al–O–Al centers). Details of the optical properties of the natural state and the change of these properties after various heat treatments between 500 and 1050 °C over different periods of time were reported by Bertelmann et al. (1985). The chemical composition of sanidine from the Eifel area is about $K_{0.86}Na_{0.14}AlSi_3O_8$ (Hofmeister and Rossman, 1984), the nominal amount of FeO being ~0.15 wt%.

Experimental details

The EPR spectra of single crystals were recorded in the X band (~9.5 GHz) and the Q band (~35 GHz) with two Varian E-line spectrometers using 100-kHz modulation over a range of external magnetic fields **B** from $B = 0$ to $B \approx 1$ T and $B = 0$ to $B \approx 2$ T, respectively. The resonance frequency was determined by a frequency counter (HP 5340A), and the magnetic field was calibrated using proton nuclear magnetic resonance. In the X-band spectrometer, the temperature of the sample could be varied between 4.2 and 295 K. In the Q-band spectrometer, it was 295 K. Single crystals we aligned on a goniometer in the spectrometer. Because of the good cleavages parallel to (001) and (010), orientation of the **a** axis parallel to the external magnetic field **B** was particularly straightforward. The crystal could be rotated within the cryostat around an axis perpendicular to **B**. The measurements at low temperatures were carried out with a continuous-flow-type cryostat of Oxford Instruments (ESR-900A). The temperature was measured with a linearized digital temperature controller (precision ±0.1 K). The crystals, in the text referred to as natural crystals, were annealed several hours at 200 °C to avoid the influence of the Al–O–Al centers on the lines at $g_{eff} \approx 2$ in the Q band.

Results

X-band spectra

A typical X-band EPR spectrum of sanidine at 295 K is shown in Figure 1. It exhibits three characteristic resonance lines, or groups of lines, at $g_{eff} \approx 7.9$, $g_{eff} \approx 4.3$, and $g_{eff} \approx 3.7$ for **B** parallel to **c***, which are assigned to

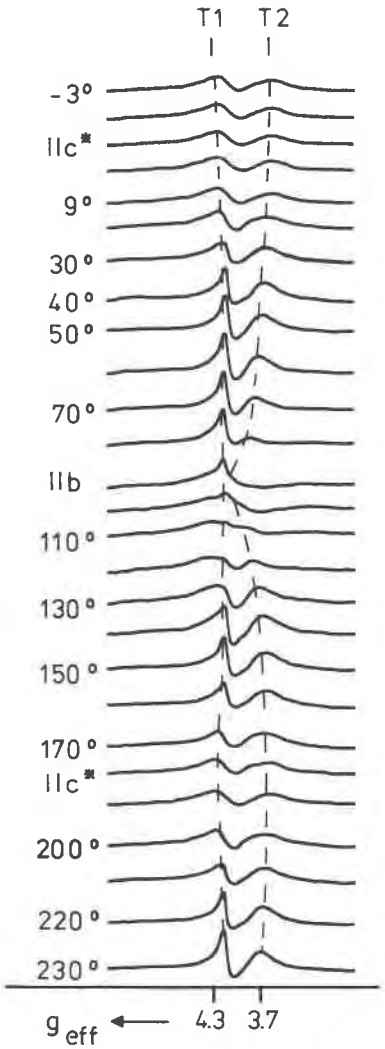

Fig. 2. EPR spectra (X band) of a natural crystal of sanidine from Volkesfeld, $\nu = 9.256$ GHz, $T = 295$ K. The crystal was rotated around **a**, which was perpendicular to **B**, **B** being in the (**c***,**b**) plane during rotation. The spectra show the assignment of the signals $g_{eff} \approx 4.3$ and $g_{eff} \approx 3.7$ to the tetrahedral positions T1 and T2, respectively, of the crystal structure of sanidine, as well as the dependency of the signals on the orientation of the crystal to **B**.

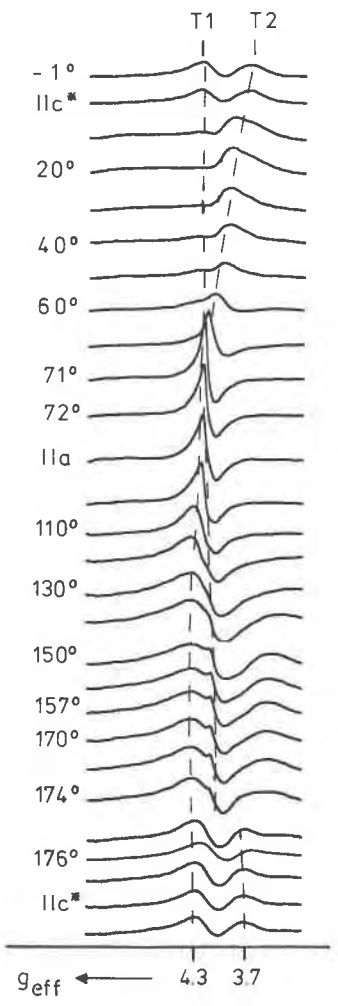

Fig. 3. EPR spectra (X band) of the crystal used also for Fig. 2. Experimental conditions and signal assignments as in Fig. 2. The crystal was rotated around **b**, **B** being in (010).

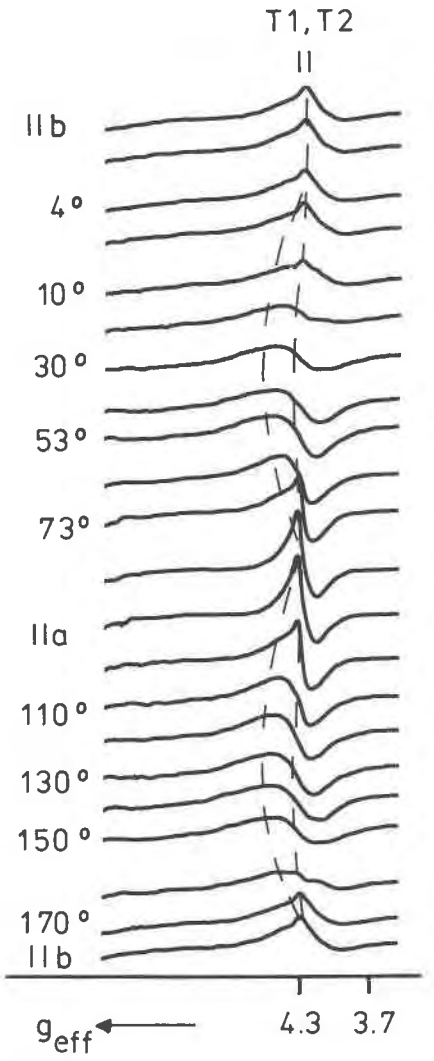

Fig. 4. EPR spectra (X band) of the crystal also used for Fig. 2. Experimental conditions and signal assignments as in Fig. 2. The crystal was rotated around **c***, **B** being in (001).

Fe^{3+}. The resonance fields of all these lines depend on the orientation of the crystal to **B**. The line $g_{eff} \approx 7.9$ varies generally between $g_{eff} \approx 6.8$ and $g_{eff} \approx 9.4$; the line $g_{eff} \approx 4.3$ is nearly "isotropic," i.e., its position is nearly invariant; and the line $g_{eff} \approx 3.7$ varies between $g_{eff} \approx 4.3$ and $g_{eff} \approx 3.7$. The widths of these lines are substantially broader than the Fe^{3+} lines in microcline or albite. They are generally quite anisotropic and vary between 0.02 and 0.05 T for different orientations. The broad line at $g_{eff} \approx 2$ cannot be assigned to Fe^{3+} at cation sites in the crystal structure. It is interpreted as a spin-spin interaction of iron oxide particles or iron clusters at interstitial positions (Aharoni and Litt, 1971; Friebele et al., 1971; Griscom, 1980; Bart et al., 1982; Calas and Petiau, 1983).

It was found that the two apparent lines at $g_{eff} \approx 4.3$ and $g_{eff} \approx 3.7$ are in fact split into more lines depending on the orientation. To investigate this in detail, the region of the spectrum between $g = 5$ and $g = 3$ was studied systematically. That region is shown in Figures 2, 3, and 4 for many different orientations of the crystal with respect to **B**. Since the lines of sanidine are 10 to 20 times broader than those of microcline or albite, the resolution of the shifts of their center positions due to a change of

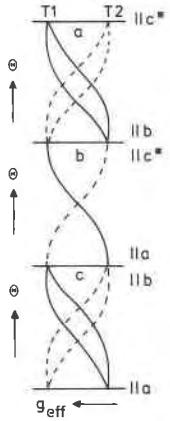

Fig. 5. Predicted splitting of EPR signals due to T1 (solid lines) and T2 (dashed lines); simplified scheme. The three rotations **a**, **b**, and **c*** correspond to the orientations described in Figs. 2, 3, and 4, respectively. Note that in rotation **b**, the signals of T1 and T2 should not split.

orientation is reduced substantially. However, the intensities of the lines are quite anisotropic; they are quite strong for certain orientations (cf., e.g., Fig. 2, ~70°) while for others they are rather weak. All spectra for the various orientations of the crystal confirm the symmetry of the monoclinic crystal class $2/m$ exactly. The principles of the observed signal splitting are demonstrated in Figure 5.

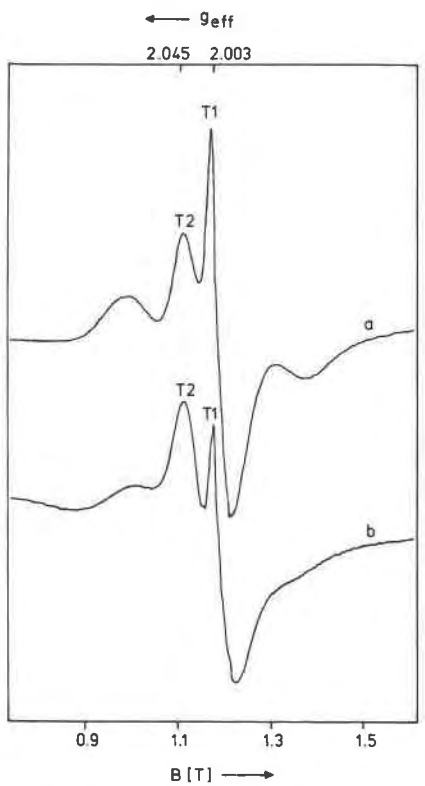

Fig. 6. EPR spectrum (Q band) of a crystal of sanidine from Volkesfeld at 295 K, **c***||**B**, ν = 35.253 GHz, (a) natural crystal, (b) crystal heated at 1050 °C for 1300 h. The assignment of the two Fe^{3+} signals to T1 and T2 is obtained from the relative change in intensity after heating, due to the somewhat more disordered distribution of Fe^{3+} over T1 and T2.

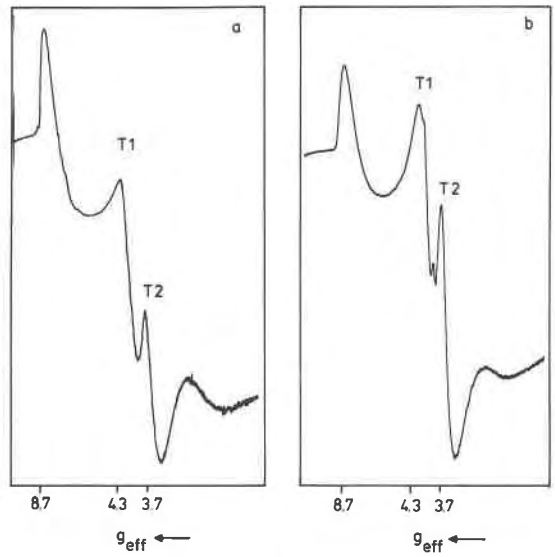

Fig. 7. EPR spectrum (X band) of a crystal of sanidine from Volkesfeld at 4.2 K, **c***||**B**, ν = 9.060 GHz, (a) natural crystal, (b) crystal heated at 1050 °C for 1300 h. In (b) the intensity of T1 is somewhat decreased compared to (a), whereas that of T2 is somewhat increased, indicating a somewhat more disordered distribution of Fe^{3+} over T1 and T2 after heating.

X-band spectra were also taken at 4.2 K for further investigation of the anisotropy of the signal intensities with respect to crystal orientation. Signal intensities are enhanced substantially at lower temperatures. The low-temperature spectra confirmed the general anisotropy at 295 K shown in Figures 2, 3, and 4 and the general signal splitting indicated in Figure 5.

Q-band spectra

Figure 6a shows a typical Q-band spectrum of sanidine at 295 K. It exhibits two strong resonance lines of Fe^{3+} at $g_{eff} \approx 2.045$ and $g_{eff} \approx 2.003$ for **B** parallel to **c***. Moreover, a very weak line exists at $g_{eff} \approx 6$ for **B** parallel to **a** (its position is out of the range of Fig. 6). Spectra of crystals oriented such that **B** was in the (**c***, **b**), (010), and (001) planes yielded quite similar characteristics as the spectra in Figures 2, 3, and 4. However, quantitative analysis is not easy since the lines show very weak angular dependencies and are overlapping in many directions.The very broad lines ($\Delta B \approx 0.3$–0.4 T) at $g_{eff} \approx 2$ may be interpreted as spin-spin interaction of very small iron oxide particles or iron clusters in the crystal, as indicated also in X-band spectra.

Heated crystals

One of the aims of this study was to obtain information on possible changes of the Fe^{3+} distribution in sanidine from the relative intensities of the signals. Because of the general anisotropy of the single-crystal spectrum of sanidine, this goal is not easily accomplished in quantitative

terms. X- and Q-band spectra of the same orientation were compared by inspection. After heating at 1050 °C for 360 h, no change in the characteristic resonance lines of Fe^{3+} could be observed either in the X or the Q band. However, a significant change was found after heating at 1050 °C for 1300 h (Figs. 6 and 7).

Discussion

Line shapes and line intensities

The typical line shape for the observed resonance signal of a single crystal is the first derivative of the absorption signal. The recorded lines of sanidine, however, are somewhat asymmetric in X- as well as Q-band spectra. They appear to be mixed with a component of absorption shape and resemble line shapes in powder spectra. We interpret the observed complex line shape to be due to local disorder around Fe^{3+} sites produced by a high degree of (Al,Si) disorder and possibly by additional defects that perturb the crystal field at the Fe^{3+} center. Small variations in the local environment of the Fe^{3+} site cause a range of different CEFs and produce deviations in the orientation of the principal axes of the **g** tensor (Scala et al., 1978; Matyash et al., 1981). Such defects may not necessarily perturb the highly perfect long-range periodicity of the crystal lattice as found from X-ray, neutron, and gamma diffraction studies by Bertelmann et al. (1985). For more details on the line shape in EPR spectra of powders, the reader is referred to Aasa (1970) and Shcherbakova and Isotomin (1975). A quantitative analysis in our case is not easy to carry out, because of background problems and broad, partly overlapping resonance lines that may be due to iron at interstitial positions and/or iron oxide particles or clusters in the crystal.

X-band spectra

The signals at $g_{eff} \approx 4.3$ and $g_{eff} \approx 3.7$ are interpreted in terms of Fe^{3+} at two distinct crystallographic positions without point symmetry that are assigned to the tetrahedral positions T1 and T2 of the monoclinic crystal structure of sanidine. Note that for certain orientations, the signals collapse to apparently one signal with increased intensity as shown in Figures 2, 3, and 4.

The general orientation dependency of the resonance fields for a paramagnetic center at positions with different symmetries was derived by Rae (1969), Weil et al. (1973), Nisamutdinov et al. (1976), and Meilman and Samoilovich (1977). A case for two distinct Fe^{3+} positions in space group $C2/m$ and point symmetry 1 is shown in Figure 5, which illustrates the splittings expected for sanidine.

Thus, for general orientations in Figure 3, two signals should be observed in our case, whereas in Figures 2 and 4, four signals should be recognized. Apparently "one intense line" may be produced by four different factors: (1) Coincidence of signals due to Fe^{3+} at equivalent sites of a position for a special orientation, each site exhibiting the same orientation with respect to **B**. (2) Accidental coincidence, or "crossing-over" of the signals due to Fe^{3+} at nonequivalent positions, e.g., T1 and T2. (3) Special orientation of the CEF splitting (the fine structure terms of Eq. 1) to **B**, e.g., one of the eigenvectors being about parallel to **B**. (4) "Mosaic effect" due to domain structure in the crystal.

TABLE 1. EPR initial field (fine structure) data of alkali feldspars

Mineral	Site	g value	Band	$\lambda = B_2^2/3B_2^0$	Ref.*
	T1(O)	2.000**	Q	0.32	a
Microcline	T1(O)	2.002†	Q	0.31	b
Albite	T1(O)	2.003††	Q	0.07	b
Glasses	—	4.3‡	X	0.33	c
Sanidine	T1	4.3§	X	0.32	d
		2.003§	Q		
	T2	3.7§	X	0.22	d
		2.045§	Q		
	FeO_3OH	5.8‖	Q	~0	d

* (a) Marfunin et al. (1967), (b) Gaite and Michoulier (1970), (c) Bershov et al. (1983), (d) this work.
** $g_x = g_y = g_z = 2.00$.
† $g_x = 1.995$, $g_y = g_z = 2.002$.
†† $g_x = g_y = g_z = 2.003$.
‡ g_{eff}.
§ g_{eff} (**B**‖**c***).
‖ g_{eff} (**B**‖**a**).

The marked increase in intensity at about 70° in Figure 2, or at about 80° in Figure 4, corresponds most probably with case 2. The unusually sharp signals in Figure 3 between 150° and 174° may be due to case 3.

The lines between $g_{eff} \approx 4.3$ and $g_{eff} \approx 3.7$ are of particular interest. A strong apparent line in this region is well known. It was reported by Sands (1955) in soda-lime-silica glass at $g_{eff} \approx 4.3$. Castner et al. (1960) assigned that glass line to a Fe^{3+} center with an axial field parameter $D = 0$, an orthorhombic field parameter $E \gg h\nu$, and a computed field value of $g = 30/7 = 4.286$. Castner et al. considered that a small D would have the effect of broadening the line at $g_{eff} \approx 4.3$.

In sodium silicate glass, Loveridge and Parke (1971) found that the line at $g_{eff} \approx 4.3$ results from a paramagnetic cluster of C_{2v} symmetry that has the form $FeO_2^AO_2^B$ (A and B label structurally nonequivalent oxygens). Brodbeck and Bukrey (1981) made analytical calculations for the magnitude of the angular and radial distribution of that cluster in oxide glasses that is required to produce the frequently observed line at $g_{eff} \approx 4.3$ in the X-band spectrum. In the Q-band spectrum, this line cannot be observed.

Using the diagrams of Gaite and Michoulier (1970; Figs. 1 and 2), $\lambda = 0.32$ and $\lambda = 0.22$ were obtained for the resonance lines at $g_{eff} \approx 4.3$ and $g_{eff} \approx 3.7$, respectively. This is indicative of a geometrical distinction of the local symmetry for Fe^{3+} at the T1 and T2 tetrahedra. Whereas Fe^{3+} at T1 ($g_{eff} \approx 4.3$, $\lambda = 0.32$) is apparently subjected to a field of "pseudo-orthorhombic" symmetry, the symmetry of T2 ($g_{eff} \approx 3.7$, $\lambda = 0.22$) is distinctly more axial. The λ values of sanidine may be compared with those of other alkali feldspars and natural acid silicate glasses in Table 1.

Bershov et al. (1983) studied EPR spectra of acid volcanic glasses and found $\lambda = 0.33$ for the respective Fe^{3+}

line at $g_{eff} \approx 4.3$. Based on the superposition model (Newman and Urban, 1975; Brodbeck and Bukrey, 1981), $Fe^{3+}O_4$ tetrahedra were considered to be embedded in a matrix of SiO_4 tetrahedra with a Si–O distance of 1.62 Å. It was possible to interpret the experimental data in terms of an FeO_4 tetrahedron (Fe–O = 1.862 Å) with a 9.3° quasi-orthorhombic distortion from cubic symmetry of the two opposite tetrahedral angles O–Fe–O. From such angular distortion, a crystal-field parameter $D = 0.42$ cm^{-1} may be computed. The crystal fields at the T1 and T2 positions of Fe^{3+} in sanidine are similar. At any rate, the magnitudes of D for sanidine are higher than 0.18 cm^{-1} since the transition $m_s = \pm 3/2$ can be observed in the X-band spectrum. The transition is assigned to correspond with the lines at $g_{eff} \approx 4.3$ and $g_{eff} \approx 3.7$. Accordingly, the line at $g_{eff} \approx 7.9$ should correspond with a $m_s = 5/2 \rightarrow m_s = 3/2$ transition.

Q-band spectra

The lines at $g_{eff} \approx 4.3$ and $g_{eff} \approx 3.7$ observed in the X band (see above) could not be found in the Q-band spectrum. This indicates that the values of D corresponding with these two lines in the X band must be in the range 0.68 cm$^{-1} \leq D \geq 0.18$ cm^{-1}. At the microwave frequencies of the Q band, the relation $D \geq 0.7$ cm^{-1} is not satisfied by radial distortion of the Newman superposition model over the full range of the distortion parameter R_1/R_0 ($1 \leq R_1/R_0 \leq \infty$) for Fe^{3+} ions with nearest oxygen ions at $R_0 = 1.95$ Å. In general the relation $D \geq 0.7$ cm^{-1} readily precludes the observation of the $g_{eff} \approx 4.3$ resonance as the microwave frequency is increased (Brodbeck and Bukrey, 1981). This result also agrees with experimental observation that the $g_{eff} \approx 4.3$ resonance disappears when the microwave frequency is increased from X band to Q band (cf., e.g., Loveridge and Parke, 1971). Gaite and Michoulier (1970) showed that a line $g \approx 2.0$ detected in alkali feldspar generally must result from the transition between states with $m_s = \pm 1/2$. The two strong signals observed in sanidine at $g_{eff} = 2.003$ and $g_{eff} \approx 2.045$ (Fig. 6) correspond with the transition $m_s = \pm 1/2$. These two lines, therefore, must also be assigned to Fe^{3+} centers at T1 and T2 positions.

An additional very weak resonance line in the Q band occurs at $g_{eff} \approx 6$ for **B** parallel to **a**, which is interpreted to be due to the transition $m_s = \pm 3/2$. This center must possess an initial field splitting $D \approx 0.68$ cm^{-1}. Friebele et al. (1971) observed in oxide semiconducting glass at 295 K a line at $g_{eff} \approx 4.3$ (X band) and at 77 K two additional lines at $g_{eff} \approx 2$ and $g_{eff} \approx 6$ (X band). In sanidine, these latter two lines could not be found throughout the whole temperature range from 4.2 to 295 K. According to the diagram of Gaite and Michoulier (1970), λ should be near zero for $g_{eff} \approx 6$, i.e., the crystal field of that Fe^{3+} site should be nearly axially symmetric. Loveridge and Parke (1971) found that in potash silicate glass contaminated with sulfur, a line at $g_{eff} \approx 6$ can be observed. The intensity of this line increases with higher contamination. The authors suggested that Fe^{3+} tetrahedra with axial symmetry result from substitution of oxygen by sulfur. A simple explanation for sanidine would be a tetrahedral Fe^{3+} site, T1 or T2, with one of the apical oxygens replaced by OH. In fact, infrared absorption spectra of sanidine from Volkesfeld yielded bands that can be attributed to OH groups attached to $(Al,Si)O_4$ tetrahedra and to molecular H_2O probably at the position of the alkali ions (Beran, 1986). The weak line at $g_{eff} \approx 6$ might be due to a $Fe^{3+}O_3OH$ tetrahedron with pseudotrigonal symmetry substituted at a T position. Lehmann (1984) reported 0.013 wt%, Hofmeister and Rossman (1985) 0.017 wt%, and Beran (1986) 0.036 wt% H_2O for the sanidine from Volkesfeld. These values would be in accord with the relative intensity of the line at $g_{eff} \approx 6$ compared to the much stronger lines of Fe^{3+} at the regular T1 and T2 sites.

Assignment of Fe^{3+} to T1 and T2

In conclusion of the discussion above and the data of Table 1, the resonance lines at $g_{eff} \approx 4.3$ and $g_{eff} \approx 3.7$ in the X-band spectrum represent transitions between levels with $m_s = \pm 3/2$ and the lines at $g_{eff} \approx 2.003$ and $g_{eff} \approx 2.045$ in the Q band between levels with $m_s = \pm 1/2$. These transitions refer to two distinct Fe^{3+} centers that must have similar polyhedral geometry. These centers are assigned to the tetrahedral positions T1 and T2, respectively, of sanidine. Because of the general broadness of the Fe^{3+} signals in sanidine, it is not possible to determine the crystallographic-orientation dependency of all signals on **B** precisely. Thus the complete initial-field-splitting tensor **D** cannot be obtained easily. The broadening of the lines is due to the local distribution of the crystalline electric field, which is caused by structural variations in the environment of the different Fe^{3+} centers. However, from the data of Table 1, it is concluded that D for the two positions is of the same order of magnitude as expected from the rather small difference in geometrical distortion of the tetrahedra. It should be noted in Table 1 that in potassium feldspars, λ at T1 in sanidine is quite similar to the value in microcline whereas λ at T2 in sanidine is somewhat smaller. The relative assignment of the signals as marked in Figures 2, 3, 4, and 5 is confirmed also by a heating experiment at 1050 °C for 1300 h. The relative changes in intensity of Fe^{3+} (T1) and Fe^{3+} (T2) on heating are shown in Figures 6a and 6b for the Q band and in Figures 7a and 7b for the X band. The somewhat more intense line in natural sanidine before heating corresponds to T1, in accord with the assumed location of Fe^{3+} at T1(O) in microcline or albite. The T1(O) or T1 position is the preferable position for Al^{3+} in alkali feldspars in general.

$Fe^{3+} \leftrightarrow Al^{3+}$ exchange

It was shown by EPR that in microcline and low albite there is only one crystallographic Fe^{3+} position. However, there is no experimental proof that Fe^{3+} most probably substitutes for Al^{3+} at the T1(O) position in those structures, because of the somewhat greater volume of the T1(O) tetrahedron compared to the T1(m), T2(O), and T2(m) tetrahedra that are occupied by Si. This preference

follows from the relative magnitudes of the ionic radii according to the sequence $Fe^{3+} > Al^{3+} > Si^{4+}$. In fact, Fe^{3+} may be substituted at Al^{3+} positions in most Al-bearing silicates and oxides, at least as a trace ion. In sanidine, Fe^{3+} occurs at T1 as well as at T2 positions. The nearly disordered distribution of Fe^{3+} observed in natural sanidine is indicative of rather slow kinetics of the $Fe^{3+} \leftrightarrow Al^{3+}$ exchange among T1 and T2 in the subsolidus range of temperatures in alkali feldspars. This was confirmed by two heating experiments at 1050 °C that were kindly carried out by Dr. H. Bernotat in Karlsruhe. Although no significant change of the relative intensities of the T1 and T2 could be observed by inspection of either the X-band or the Q-band spectra after heating at 1050 °C for 360 h, a relative increase in intensity of the T2 signal was detected after heating at the same temperature for 1300 h. More quantitative details of the kinetics are still open, but it appears that the $Fe^{3+} \leftrightarrow Al^{3+}$ as well as $Fe^{3+} \leftrightarrow Si^{4+}$ exhanges are comparable, or even slower than the $Al^{3+} \leftrightarrow Si^{4+}$ exchange. Wones and Appleman (1961, 1963) found that synthetic $KFe^{3+}Si_3O_8$ (microcline structure) is triclinic and well ordered. It appears to remain ordered as temperature and pressure are increased until a phase transition to a monoclinic phase occurs at 704 °C and 2 kbar. Intermediate stages of partial (Fe^{3+},Si^{4+}) disorder could not be detected. The transition temperature is significantly (more than 100 °C) higher than that of microcline to sanidine.

It would be interesting to compare the Al and Si site occupancies obtained from accurate determinations of the lattice constants with EPR spectra of the same heat-treated crystal. There is no information on whether it is possible to obtain potassium feldspar more ordered in Fe^{3+}, e.g., by hydrothermal recrystallization.

Acknowledgments

We thank Drs. L. V. Bershov, IGEM, Academy of Sciences of USSR, Moscow, USSR, J.-M. Gaite, Université d'Orléans, France, and G. Lehmann, Universität Münster, West Germany, for many helpful discussions. Drs. H. Bernotat and H. Wondratschek, Technische Universität Karlsruhe, West Germany, kindly supplied the sanidine crystals and carried out the heating experiments. The X-Band EPR spectrometer was financed by the U.S. National Science Foundation under Grant Ga 14811 and the Q-Band EPR spectrometer by the Deutsche Forschungsgemeinschaft under Grant SFB-127.

References cited

Aasa, R. (1970) Powder line shapes in the electron paramagnetic resonance spectra of high-spin ferric complexes. Journal of Chemical Physics, 52, 3919–3930.

Aharoni, S.M., and Litt, M.H. (1971) Superparamagnetism and exchange anisotropy in microparticles of magnetite embedded in an inert carbonaceous matrix. Journal of Applied Physics, 42, 352–356.

Bank, H. (1967) Hellbrauner klar durchsichtiger Alkalifeldspat von Volkesfeld-Eifel. Zeitschrift der Deutschen Gesellschaft für Edelsteinkunde, 61, 50–53.

Bart, J.C.J., Burriesci, N., Cariati, F., Cavallaro, S., Giordano, N., and Petrera, M. (1982) Nature and distribution of iron in volcanic glass: Mössbauer and EPR study of Lipari pumice. Bulletin de la Société Française de Minéralogie et de Cristallographie, 105, 43–50.

Beran, A. (1986) A model of water allocation in alkali feldspar, derived from infrared-spectroscopic investigations. Physics and Chemistry of Minerals, 13, 306–310.

Bershov, L.V., Marfunin, A.S., Mineeva, R.M., and Nasedkin, V.V. (1983) Über die stabilisierende Rolle des Eisens in der Struktur von natürlichen Gläsern. Dokladii Akademii Nauk SSSR, 268, 960–963.

Bertelmann, D., Förtsch, E., and Wondratschek, H. (1985) Zum Temperverhalten von Sanidinen: Die Ausnahmerolle der Eifel sanidin-Megakristalle. Neues Jahrbuch für Mineralogie Abhandlungen 152, 123–141.

Brodbeck, C.M. (1980) Investigations of g value correlations associated with the $g = 4.3$ ESR signal of Fe^{3+} in glass. Journal of Non-Crystalline Solids, 40, 305–313.

Brodbeck, C.M., and Bukrey, R.R. (1981) Model calculations for the coordination of Fe^{3+} and Mn^{2+} ions in oxide glasses. Physical Review B, 24, 2334–2342.

Calas, G., and Petiau, J. (1983) Structure of oxide glasses: Spectroscopic studies of local order and crystallochemistry. Geochemical implications. Bulletin de la Société Française de Minéralogie et de Cristallographie, 106, 33–55.

Castner, Th., Newell, G.S., Holton, W.C., and Slichter, C.P. (1960) Note on the paramagnetic resonance of iron in glass. Journal of Chemical Physics, 32, 668–673.

Dowsing, R.D., and Gibson, J.F. (1969) Electron spin resonance of high-spin d^5 systems. Journal of Chemical Physics, 50, 294–303.

Frechen, J. (1976) Siebengebirge am Rhein-Laacher Vulkangebiet-Maargebiet der Westeifel. Sammlung Geologischer Führer 56. Borntraeger, Berlin.

Friebele, E.J., Wilson, L.K., Dozier, A.W., and Kinser, D.L. (1971) Antiferromagnetism in an oxide semiconducting glass. Physica Status Solidi (b), 45, 323–331.

Gaite, J.M., and Michoulier, J. (1970) Application de la résonance paramagnétique électronique de l'ion Fe^{3+} à l'étude de la structure des feldspaths. Bulletin de la Société Française de Minéralogie et de Cristallographie, 93, 341–356.

Griscom, D.L. (1980) Electron spin resonance in glasses. Journal of Non-Crystalline Solids, 40, 211–272.

Hofmeister, A.M., and Rossman G. (1984) Determination of Fe^{3+} and Fe^{2+} concentrations in feldspar by optical absorption and EPR spectroscopy. Physics and Chemistry of Minerals, 11, 213–224.

——— (1985) A model for the irradiative coloration of smoky feldspar and the inhibiting influence of water. Physics and Chemistry of Minerals, 12, 324–332.

Hutton, G.J. (1969) Rotational properties of electron spin resonance spectra. Journal of Physics C, 2, 673–679.

Lehmann, G. (1984) Spectroscopy of feldspars. In W.L. Brown, Ed. Feldspars and feldspathoids, NATO ASI Series C 137, p. 121–162. D. Reidel, Dordrecht.

Loveridge, D., and Parke, S. (1971) Electron spin resonance of Fe^{3+}, Mn^{2+}, and Cr^{3+} in glasses. Physics and Chemistry of Glasses, 12, 19–27.

Marfunin, A.S. (1979) Spectroscopy, luminescence and radiation centers in minerals. Springer-Verlag, Berlin.

Marfunin, A.S., Bershov, L.V., Meilman, M.L., and Michoulier, J. (1967) Paramagnetic resonance of Fe^{3+} in some feldspars. Schweizerische Mineralogische und Petrologische Mitteilungen, 47, 13–20.

Matyash, V.I., Bagmut, N.N., Litovchenko, C.A., and Proshko, Ya.V. (1981) Anwendung der EPR-Daten von Fe^{3+} zur Bestimmung von Strukturbesonderheiten der Alkalifeldspäte. Mineralogicheskii Zhurnal, 3, 76–80.

Meilman, M.L., and Samoilovich, M.I. (1977) Einführung in die EPR-Spektroskopie. Atomisdat, Moskwa.

Michoulier, J., and Gaite, J.M. (1972) Site assignment of Fe^{3+} in low symmetry crystals. Application to $NaAlSi_3O_8$. Journal of Chemical Physics, 56, 5205–5213.

Newman, D.J., and Urban, W. (1975) Interpretation of S-state ion EPR spectra. Advances in Physics, 24, 793–844.

Nisamutdinov, N.M., Bulka, G.R., Gainullina, N.M., and Vinokurov, V.M. (1976) Symmetrie der Defektverteilung in Punktsystemen und Eigenschaften der Richtungsabhängigkeit von EPR-Spektren in Kristallen. Fisicheskie svoistva mineralov i gornih porod. Ed. Universität Kazan.

Rae, A.D. (1969) Relationship between the experimental Hamiltonian and the point symmetry of a paramagnetic species in a crystal. Journal of Chemical Physics, 50, 2672–2685.

Sands, R.H. (1955) Paramagnetic resonance absorption in glass. Physical Review, 99, 1222.

Scala, C.M., Hutton, D.R., and McLaren, A.C. (1978) NMR and EPR studies of the chemically intermediate plagioclase feldspars. Physics and Chemistry of Minerals, 3, 33–44.

Shcherbakova, M.Ya., and Istomin, E.V. (1975) Calculation of EPR spectra of Fe^{3+} with high zero-field splitting in polycrystalline materials. Physica Status Solidi (b), 67, 461–469.

Speit, B., and Lehmann, G. (1982) Radiation defects in feldspars. Physics and Chemistry of Minerals, 8, 77–82.

Troup, G.J., and Hutton, D.R. (1964) Paramagnetic resonance of Fe^{3+} in kyanite. British Journal of Applied Physics, 15, 1493–1499.

Weil, J.A., Buch, T., and Clapp, J.E. (1973) Crystal point group symmetry and microscopic tensor properties in magnetic resonance spectroscopy. Advances in Magnetic Resonance, 6, 183–257.

Wickman, H.H., Klein, M.P., and Shirley, D.A. (1965) Paramagnetic resonance of Fe^{3+} in polycrystalline ferichrome A*. Journal of Chemical Physics, 42, 2113–2117.

Wones, D.R., and Appleman, D.E. (1961) X-ray crystallography and optical properties of synthetic monoclinic $KFeSi_3O_8$ iron-sanidine. U.S. Geological Survey Professional Paper 424-C, C309–C310.

——— (1963) Properties of synthetic triclinic $KFeSi_3O_8$, iron-microcline, with some observations on the iron-microcline–iron-sanidine transition. Journal of Petrology, 4, 131–137.

Manuscript received August 28, 1986
Manuscript accepted September 2, 1987